

Cloaking devices: progress with metamaterials

Graham C. Holt

Collegium Basilea (Institute of Advanced Study), Basle, Switzerland

Since the practical realization of negative refractive index materials in 2001, considerable progress has been made in both designing the materials and extending the range of the electromagnetic spectrum that may be manipulated. This paper reviews progress, especially in the field of visible light and the applications to cloaking devices, lenses and switches.

1. Introduction

Metamaterials with negative refractive index capable of bending electromagnetic waves back towards the transmitter and offering the possibility of cloaking devices first gained popular prominence around 2001 after a practical demonstration¹ of Pendry's theoretical calculations.² At that time, the microstructured metamaterial was effective in the radar spectrum and it was already evident then that crystalline structures and nanomaterials would soon extend negative refractive index into the visible spectrum.³ Hopes of cloaking aircraft or vehicles appealed to science fiction fans but the reality was (and is) still some way into the future. Nevertheless, considerable progress has been made and it is now possible, with suitable metamaterials, to bend electromagnetic waves round an object across much of the spectrum. Other predicted applications such as fast optical switches and superlenses have now found some application but 10 years on there is still little evidence of the subject's practical use.

2. Theory and limitations

The wave solution to Maxwell's equations at an interface gives rise to Snell's law of refraction, derived by assuming continuity of the wave function across the interface:

$$n_1 \sin(\theta_1) = n_2 \sin(\theta_2), \quad (1)$$

¹ R.A. Shelby, D.R. Smith and S. Schultz. Experimental verification of a negative index of refraction. *Science* **292** (2001) 77–79.

² G. Guida, P.N. Stavrinou, G. Parry and J.B. Pendry. Time-reversal symmetry, microcavities and photonic crystals. *J. Modern Optics* **48** (2001) 581–595.

³ G.C. Holt. Negative index of refraction and metamaterials. *Nanotechnology Perceptions* **4** (2008) 201–205.

where n is the refractive index,

$$n = (\epsilon\mu)^{1/2}, \quad (2)$$

where ϵ is the permittivity and μ is the magnetic permeability. With n taken as the negative square root if ϵ and μ are both negative, then the electromagnetic wave of the light is bent outwards rather than inwards, see Figure 1.

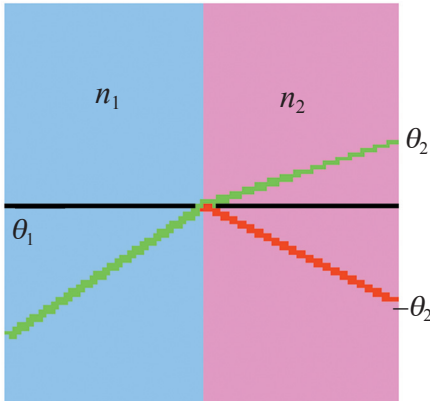


Figure 1. Snell's law at the interface of two materials with refractive indices n_1 and n_2 . Green is the normally refracted ray while the red ray results from one material having negative refractive index. θ_1 is the angle of incidence and θ_2 the angle of refraction.

Initial calculations of negative refractive index were achieved by solving Maxwell's equations for a plane wave incident on a metamaterial. In its simplest form, the **E** field interacts with a simple resonant circuit in a metamaterial to produce a complex permittivity. This involves solving both Maxwell's equations and Drude's model for electron motion to determine the current in the metamaterial and thus permittivity. In these simple models the permittivity, both electric and magnetic, are functions only of the frequency of the incident electromagnetic wave and the structure of the metamaterial, i.e. the average time between electron collisions with the material's ions.

Maxwell's equations are:

$$\nabla \wedge \mathbf{E} = -c^{-1} \partial_t \mathbf{B}, \quad (3)$$

$$\nabla \wedge \mathbf{H} = c^{-1} \partial_t \mathbf{D} + 4\pi \mathbf{j}, \quad (4)$$

$$\mathbf{D} = \epsilon \mathbf{E}, \quad (5)$$

$$\mathbf{B} = \mu \mathbf{H} \quad (6)$$

where **E** and **H** are the electric and magnetic fields, and **D** and **B** are the dielectric displacement and magnetic inductive fields, respectively. The current density **j** and the speed of light is c .

The wave solution for the equations is given by

$$\mathbf{E} = \mathbf{K} \wedge \mathbf{H}_0 e^{i(\mathbf{K} \cdot \mathbf{x} - \omega t)}, \quad (7)$$

$$\mathbf{H} = \mathbf{K} \wedge \mathbf{E}_0 e^{i(\mathbf{K} \cdot \mathbf{x} - \omega t)} \quad (8)$$

where **K** is the phase propagation direction and ω the angular frequency, provided

$$\mathbf{K} = \frac{\omega n}{c} \hat{\mathbf{K}}, \quad (9)$$

where $\hat{\mathbf{K}}$ is the unit vector. Note that the energy flux or Poynting vector is given by

$$\mathbf{P} = \mathbf{E} \wedge \mathbf{H} \propto \mathbf{K}. \quad (10)$$

Thus, \mathbf{E} , \mathbf{H} and \mathbf{K} form a right-handed vector space provided n is greater than zero. If n is less than zero then this becomes a *left-handed vector space*, which has given rise to the term “left-handed materials” (which exhibit negative refractive index). Negative refractive index also then gives backward Cerenkov radiation and reversed Doppler shift.

Drude's model of electrons in the conduction band of a material is given by

$$\partial \mathbf{p} = q[\mathbf{E} + \mathbf{p} \wedge \mathbf{H}m^{-1}] - \mathbf{p}\tau^{-1}, \quad (11)$$

where \mathbf{p} is the charge momentum, q the charge ($= -e$), m is the electron mass and τ is the time between electron collisions with the ions in the crystal structure of the electrons. The current density is given by

$$\int \mathbf{j} \partial V = v q \mathbf{p} / m, \quad (12)$$

where v is the number of charge carriers.

Solving equations 11 and 12 in the presence of a time-dependent \mathbf{E} then gives the permittivity, in the form

$$\epsilon = 1 + \frac{\omega_p^2}{\omega_0^2 - \omega^2 - i\omega\Gamma}, \quad (13)$$

where the metal plasma frequency, at which the metal becomes transparent, is

$$\omega_p^2 = \frac{4\pi Ne^2}{m^*}, \quad (14)$$

while N is the carrier density and m^* the effective mass of the charge carriers.

More recent developments involving nanostructured materials have meant that the permittivity is a function of not only frequency but also the position in the material. This has meant, in practice, that computer modelling has been required to solve the equations. Nevertheless, it is now almost possible to design a nanostructured material to achieve a given negative refractive index.

Perhaps the most attractive feature of negative refractive index is the fact that the evanescent field of the electromagnetic wave may be refocused producing a “superlens” (See section 5) with resolution better than the diffraction limit. As a wave propagates through a conventional material, slow velocity components are attenuated and lost, which gives rise to the diffraction limit of resolution. The negative refractive index effectively refocuses these evanescent waves, allowing resolution to a fraction of the incident wavelength. From equation (9), a wave travelling in the z direction has wave vector

$$\mathbf{K}_z = \left[\left(\frac{\omega n}{c} \right)^2 - \mathbf{K}_x^2 - \mathbf{K}_y^2 \right]^{1/2}, \quad (15)$$

so that \mathbf{K}_x and \mathbf{K}_y are imaginary and are attenuated. The diffraction limit is the case

$$\mathbf{K}_z \approx \frac{\omega n}{c}, \quad (16)$$

or $\delta z \approx$ wavelength λ .

3. Metamaterials

The underlying mechanism of permittivity depends on the energy or wavelength of the incident photons. In translucent material some of the photon energy is absorbed while most is transmitted at a refracted angle given by Snell's law (equation 1). For long-wavelength radiation to near-microwave frequencies, the incident radiation creates atomic dipole moments, which heat the material and reduce the phase velocity. At higher frequencies, microwave to ultraviolet, wavelengths to about 100 nm, the electrons in the atoms and molecules of the material absorb energy by being raised to higher energy bands; as in, for example, microwave heating of water. Note the visible spectrum covers wavelengths 750–380 nm; in this region the refractive index may be a function of the wave direction due to plasmon resonance. Here the photon interaction with the solid molecule's surface electrons in the solid/air interface results in resonance. The electron oscillation in the Coulomb field of the nuclei is enhanced in the propagation direction parallel to the interface and thus is very dependent on the incident photon direction relative to the solid surface.

At very high frequencies, far ultraviolet to X-rays, wavelength $\sim 10^{-3}$ nm, the atomic structure acts as a diffraction grating and Snell's law is inappropriate.

The first negative refraction index materials were constructed in the year 2000 using substrate micromachining techniques to control the electromagnetic field at microwave frequencies (a wavelength of centimetres). Now nonmagnetic media have a dielectric tensor that is extremely anisotropic and cannot be found in nature at optical frequencies. These metamaterials, typically doped crystals, operating near the plasma frequency, are functions of \mathbf{K} space, see equation (15), so that the isofrequency curve of the medium is hyperbolic as opposed to circular as in conventional media. The fundamental property of the "hyperbolic metamaterials" is that they have dielectric properties ($\epsilon \geq 0$) in one direction but metallic properties ($\epsilon \leq 0$) in an orthogonal direction.

There has been considerable progress in the design and fabrication of metamaterials available across most of the spectrum, see Figure 2.⁴

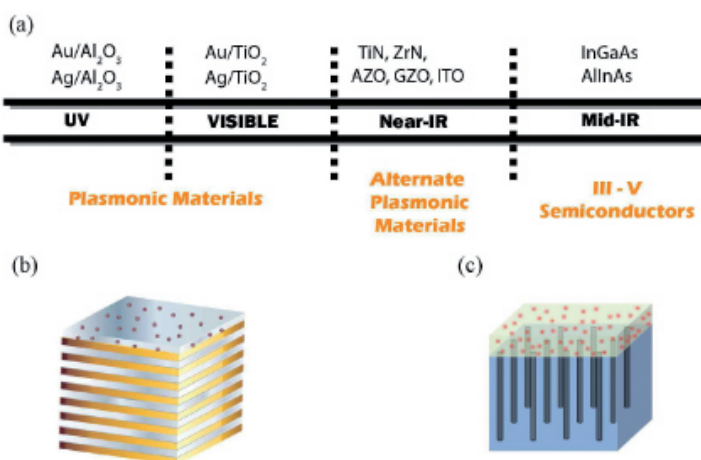


Figure 2. Metamaterial types effective across the spectrum: (a) Hyperbolic metamaterials made by a variety of plasmonic materials tailored to different regions of the electromagnetic spectrum from the visible to midinfrared frequencies; (b) multilayer realization consisting of alternating subwavelength layers of metal and dielectric; (c) Hyperbolic metamaterials based on metal nanowires in a dielectric host.

⁴ C.L. Cortes et al. Quantum nanophotonics using hyperbolic metamaterials. arXiv:1204.5529v2 [physics.optics], September 2013.

It is calculated that the combination of a waveguide utilizing plasmon resonance and a split ring resonator structure generating dipoles will in theory give negative refractive index in the visible region with a 200 nm bandwidth.⁵

However, the greatest achievements so far are still on the edge of the visible spectrum in the far infrared where a 500 nm bandwidth has been achieved using a “fishnet” design principle. A polyimide pane subdivided into many cells (like a fishing net) has demonstrated negative refractive index with good transmission properties; the cells, some 2000 nm square, have a thin layer of gold patterned with features of the order of 200 nm.⁶

4. Cloaking

Early cloaking attempts were in the radar spectrum but visible cloaking has now become a possibility. For instance, hiding a 2 mm target using blue, green and red light around 570 nm was achieved in 2011.⁷

These cloaking devices are rigid materials (cf. a rug laid over a bump) capable of making an object undetectable by visible light. The cloak was fabricated from a silicon nitride waveguide on a specially developed nanoporous silicon oxide substrate with a very low refractive index. The fabricated device demonstrated wideband invisibility throughout the visible spectrum with low loss.⁸

More flexible metamaterials are now appearing and offer the possibility, in the future, of a real invisibility cloak. A trilayer of flexible metamaterials working in the near-infrared régime can be fabricated on a transparent polyethylene terephthalate (PET) substrate using “flip chip” transfer techniques. The metamaterial device can be transformed into various shapes by bending the plastic PET substrate.⁹

Recently, rather than cloaking a whole object in the visible spectrum, the creation of an illusion has gained interest: the aim is not to hide a target but rather to create the illusion that it is in a different place. This is somewhat easier to engineer than trying to create a material that bends the light around the whole target. The process involves defining the coordinate transformation required to create the illusion and then using the Jacobian of the transformation as the definition of the real part of the refractive index of the metamaterial in wave vector space. A suitable metamaterial can then be designed. A recent example uses a photoelastic dielectric to achieve an apparent target position either up or down so that the displacement created by the illusion can be controlled by compression of the metamaterial.¹⁰

Two approaches are showing promise for the future. The first, using white light and an optical glass construction, can make large objects invisible from certain angles. To preserve the phase of the wave, previous cloaking solutions proposed by Pendry et al. required transforming

⁵ A.C. Atre et al. A broadband negative index metamaterial at optical frequencies. *Advanced Optical Materials* **1** (2013) 327–333.

⁶ Z.H. Jiang et al. Tailoring dispersion for broadband low-loss optical metamaterials using deep-subwavelength inclusions. *Scientific Reports* **3** (2013) article number 1571.

⁷ B. Zhang et al. Macroscopic invisibility cloak for visible light. *Phys. Rev. Lett.* **106** (2011) 033901.

⁸ M. Gharghi et al. A carpet cloak for visible light. *Nano Lett.* **11** (2011) 2825–2828.

⁹ G.X. Li et al. Highly flexible near-infrared metamaterials. *Optics Express* **20** (2012) 397–402.

¹⁰ D. Gao et al. Macroscopic broadband optical escalator with force-loaded transformation optics. *Optics Express* **21** (2013) 796–803.

electromagnetic space around the hidden object in such a way that the rays bending around it have to travel much faster than those passing it by. The difficult phase preservation requirement is the main obstacle for building a broadband, polarization-insensitive cloak for large objects. Abolishing the requirement for phase preservation for observation in incoherent natural light, since human eyes are phase- and polarization-insensitive, allows the cloak to be made on a large scale using commonly available materials.¹¹

The second approach uses active metamaterials to overcome the bandwidth restrictions. Using broadband, ultrathin cloaks of negatively capacitive metasurfaces, actively frequency-selective and made conformal to the object, it is calculated that it is possible to drastically reduce the scattering over a wide frequency range in the microwave régime to the extent of being orders of magnitude broader than any available passive cloaking technology.¹²

5. Superlenses

One of the earliest demonstrations of the superlens was in 2007 using a metamaterial lens consisting of gold and aluminium oxide layers, which achieved a resolution of 125 nm with 365 nm light—a third of the diffraction limit. The hyperlens consisted of 8 pairs of Ag (35 nm)/Al₂O₃ (35 nm) layers on a curved quartz mould, see Figure 3. The two line objects (on a 50 nm Cr film) are gradually magnified along the radial direction under polarized 365 nm light.¹³

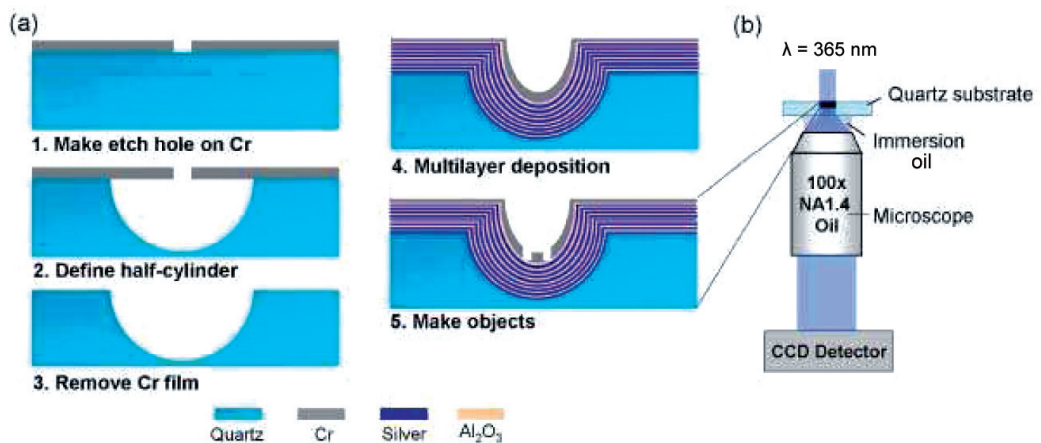


Figure 3. Superlens microscope: (a) Hyperlens sample fabrication process flow. Through the etch hole in a Cr film (1), isotropic wet etching makes a cylindrical groove in quartz (2). After the Cr film is removed (3), a multilayer hyperlens structure is fabricated using alternate deposition of Ag and Al₂O₃ (4). A Cr film caps the hyperlens structure for object fabrication so that the object is effectively part of the lens structure (5). (b) Imaging setup: the completed hyperlens/object sample is placed under a source of incident light at 365 nm; a conventional far-field microscope with a 100 × oil immersion objective and a UV-sensitive CCD detector was used for direct far-field imaging.

¹¹ H. Chen, B. Zheng et al. Ray-optics cloaking devices for large objects in incoherent natural light. *Nature Communications* **4** (2013) article number 2652.

¹² P.-Y. Chen et al. Broadening the cloaking bandwidth with non-foster metasurfaces. *Phys. Rev. Lett.* **111** (2013) 233001.

¹³ H. Lee, Z. Liu et al. Development of optical hyperlens for imaging below the diffraction limit. *Optics Express* **15** (2007) 15886–15891.

Recent proposals include an alternating graphene/dielectric multilayer-based optical hyperlens for far field subdiffraction imaging at mid-infrared frequencies. Simulation results demonstrate that two point sources with separation far below the diffraction limit can be magnified by the system to the extent that conventional far field optical microscopy can further manipulate it. Such a hyperlens has the advantage of operating in a wide band region due to the tunability of graphene's dielectric permittivity as opposed to previous metal-based hyperlenses.¹⁴

One of the most impressive superlens claims¹⁵ is that for a planar slab of negative index perovskite material in the mid-infrared régime achieving imaging resolution of $\lambda/14$. However, the imaging is complex, using an atomic force microscope (AFM) probe and the harmonics of the evanescent field.

The first practical demonstration of the superlens could be later in 2014 as a spin-off company markets a metamaterial for broadband satellite communication.¹⁶ It is instructive to note that an optical metamaterials programme¹⁷ has been organized in America, with the specific aim of creating coatings for improved solar cell efficiency, microlenses for LEDs, optical traps and delay lines for quantum computing and, of course, subwavelength optical microscopy.

6. Discussion

The concept of cloaking devices seemed to capture the public's imagination around the year 2000 and since then considerable financial support has been given to research efforts, especially by the US military through DARPA and, in the UK, the £4.9 M granted to Imperial College in 2009. Research into the underlying metamaterials has been prolific and they use in superlenses for enhanced optical microscope would seem to be not far off.

In the field of cloaking devices there are still many problems to be overcome, not least of which is the need for broad-spectrum response with a good transmissibility. A cloaking device that hides the target but shows a region of opaque background image is hardly effective. The other problem for any practicable device is the need to be able to see out, which either requires directions for which cloaking is not effective or a means of switching the metamaterial off; active metamaterials would appear to be the future in this area.

¹⁴ T. Zhang et al. Graphene-based tunable broadband hyperlens for far-field subdiffraction imaging at mid-infrared frequencies. *Optics Express* **21** (2013) 20888–20899.

¹⁵ S.C. Kehr et al. Near-field examination of perovskite-based superlenses and superlens-enhanced probe-object coupling. arXiv:1103.5032 [physics.optics], 25 March 2011.

¹⁶ L. Billings. Exotic optics: Metamaterial world. Engineered structures with bizarre optical properties are set to migrate out of the laboratory and into the marketplace. *Nature* **500** (2013) 138–140.

¹⁷ The Optical Metamaterials Program was initiated at Oak Ridge National Laboratory (ORNL) in 2009.

